

pH Jump Studies of the Folding of the Multidomain Ribosomal Protein L9: The Structural Organization of the N-Terminal Domain Does Not Affect the Anomalous Slow Folding of the C-Terminal Domain[†]

Satoshi Sato,[‡] Donna L. Luisi,[‡] and Daniel P. Raleigh^{*,‡,§}

Department of Chemistry, State University of New York at Stony Brook, Stony Brook, New York 11794-3400, and Graduate Program in Biophysics and Graduate Program in Molecular and Cellular Biology, State University of New York at Stony Brook, Stony Brook, NY 11794

Received November 10, 1999; Revised Manuscript Received February 17, 2000

ABSTRACT: The folding kinetics of the multidomain ribosomal protein L9 were studied using pH jump stopped-flow fluorescence and circular dichroism (CD) in conjunction with guanidine hydrochloride (GdnHCl) jump stopped-flow CD experiments. Equilibrium CD and 1D ¹H NMR measurements demonstrated that the C-terminal domain unfolds below pH 4 while the N-terminal domain remains fully folded. Thus, the N-terminal domain remains folded during the pH jump experiments. The folding rate constant of the C-terminal domain was determined to be 3.5 s⁻¹ by pH jump experiments conducted in the absence of denaturant using stopped-flow CD and fluorescence. CD-detected GdnHCl jump measurements showed that the N- and C-terminal domains fold independently each by an apparent two-state mechanism. The folding rate constant for the N-terminal domain and the C-terminal domain in the absence of denaturant were calculated to be 760 and 4.7 s⁻¹, respectively. The good agreement between the pH jump and the denaturant concentration jump experiments shows that the folding rate of the C-terminal domain is the same whether or not the N-terminal domain is folded. This result suggests that the slow folding of the C-terminal domain is not a consequence of unfavorable interactions with the rest of the protein chain during refolding. This is an interesting result since contact order analysis predicts that the folding rate of the C-terminal domain should be noticeably faster. The folding rate of the isolated N-terminal domain was also measured by stopped-flow CD and was found to be the same as the rate for the domain in the intact protein.

Understanding the mechanism of protein folding remains one of the major challenges in protein science. Although the information required for a protein to fold to its unique native conformation is apparently encoded in the amino acid sequence (1), it is currently impossible to accurately predict the native structure from its primary sequence. The difficulty of the prediction arises in part from an astronomically large number of different conformations that a protein can adopt and from the complexity of the free-energy landscape of protein folding, for example, local minima on the free energy surface (2, 3). Nevertheless, studies of the folding kinetics of small single-domain proteins have successfully characterized the rate-limiting step of the folding reaction and have revealed that many single-domain proteins fold without forming any detectable intermediates (4). Of particular interest have been attempts to correlate folding kinetics with properties of the native state (5, 6). The folding and assembly of multidomain proteins are, however, less well characterized.

The ribosomal protein L9, shown in Figure 1, is an interesting model system to study the folding of a multidomain protein. The structure, in which the two globular domains are connected by a rigid linker, can be viewed as an intermediate case between a protein having extensive interdomain contacts and a protein with domains connected by a flexible linker (7–9). Comparison of the folding kinetics of the isolated domains with the intact protein can also provide information about the folding of single-domain proteins. The structure has been shown to be preserved in solution, and the long central helix can fold independently (10, 11). The protein contains an rRNA-binding site in each domain and functions as a structural protein in the large subunit of the ribosome. L9 has been hypothesized to serve as a molecular strut helping maintain the conformation of rRNA (10, 12, 13). L9 provides a simple and convenient system for folding studies since it lacks disulfide bonds and does not bind to any metal ions or cofactors. The isolated N-terminal domain has been shown to retain a similar structure and stability as the domain in the intact protein. The domain folds very rapidly, on the millisecond time scale, by a two-state mechanism (14–16). There are only several other proteins that fold faster than the isolated N-terminal domain (17–22).

In this study, we combine guanidine hydrochloride (GdnHCl)¹ jump CD-detected stopped-flow measurements

[†] This work was supported by a grant from NSF (MCB-9600866) to D.P.R. who is a Pew Scholar in the Biomedical Sciences. D.L.L. was supported in part by a GAANN fellowship from the Department of Education.

* To whom correspondence should be addressed. Phone: (631) 632-9547. Fax: (631) 632-7960. E-mail: DRaleigh@notes.cc.sunysb.edu.

[‡] Department of Chemistry.

[§] Graduate Program in Biophysics and Graduate Program in Molecular and Cellular Biology.

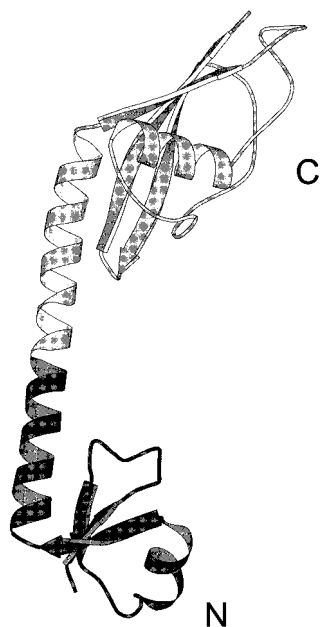


FIGURE 1: Ribbon diagram of L9 from *Bacillus stearothermophilus*. The N-terminal domain, consisting of residues 1–56 is shaded. The program MOLSCRIPT (33) was used to create this diagram.

with fluorescence and CD-detected pH jump experiments of the folding of L9. This work complements and extends our previously reported fluorescence-detected GdnHCl jump measurements. These experiments suggested that the folding of the C-terminal domain is 2–3 orders of magnitude slower than the folding of the N-terminal domain. We also use stopped-flow CD to monitor the folding of the isolated N-terminal domain of L9.

Baker and co-workers have demonstrated a correlation between the folding rates of single-domain proteins and the average separation between contacting residues as measured by the relative contact order. The relative contact order is a one parameter measure which reflects the relative importance of local and nonlocal interaction to a protein's native state (5). Topologically simple proteins having more local interactions relative to nonlocal interactions, and hence a lower relative contact order, were observed to fold faster. Recent theoretical work from Goddard and co-workers describes another scheme for predicting folding rates, which leads to somewhat different results than the contact order analysis (6). Interestingly, the two methods predict similar folding rates for the N-terminal domain of L9 but very different folding rates for the C-terminal domain of L9. The analysis of Goddard predicts a folding rate closer to the experimental value (6). The folding rate of the C-terminal domain of L9, in the intact protein, exhibits one of the largest deviations from the rate predicted by the contact order. The folding rate for the C-terminal domain predicted by the contact order analysis deviates from that observed experimentally by a factor of 35–100. (Plaxco and Kuhlman, personal communication). The relative contact order of residues 74–149, which includes the globular C-terminal domain but excludes all residues from the central helix, is 16%, and the predicted folding rate is 130 s^{-1} . Several residues from the central helix contribute to the core of the C-terminal domain. Extending

the sequence to include these lowers the relative contact order and leads to a faster predicted folding rate and an even greater deviation. The relative contact order of residues 62–149 is 14.9% corresponding to a predicted rate of 340 s^{-1} . These are among the very largest reported deviations between measured and predicted rates. The disagreement might be explained if the domain folds slower in the intact domain because of unfavorable interactions with the rest of protein during the folding. A major goal of this work is to study the effect of structure in the N-terminal domain on the folding kinetics of the C-terminal domain. We wish to determine if the rate at which the C-terminal domain folds is influenced by the presence of a folded N-terminal domain. In some cases, domains derived from multidomain proteins fold faster in isolation than when they are part of the intact protein (23, 24), suggesting that there may be unfavorable interactions with the rest of the peptide chain during the folding of a domain. This possibility can be tested for the case of L9 by comparing pH jump experiments to denaturant jump experiments. The C-terminal domain unfolds at low pH while the N-terminal domain remains fully folded. In pH jump experiments, the N-terminal domain remains folded, and it is unlikely that there is any interference with the rest of the protein during the folding of the C-terminal domain.

A second important goal of the present study is to examine the folding kinetics of L9 using a probe which reports on secondary structure formation. Our previous studies have made use of fluorescence-detected stopped-flow. Each of the domains contains a single tyrosine residue which serves as a convenient spectroscopic marker of the local environment near these residues. The fluorescence measurements were consistent with the two-state folding of each domain (25). Comparison of the stopped-flow CD results presented here with our previous fluorescence measurements offers an excellent and more rigorous test of the apparent two-state nature of the folding transitions.

Finally, the folding kinetics of two variants of the isolated N-terminal domain are compared to the domain in the intact protein. An interesting correlation between the stability of the N-terminal region and the position of the transition state for folding is noted.

MATERIALS AND METHODS

Expression and Purification of L9. The ribosomal protein L9 from *Bacillus stearothermophilus* was expressed and purified by the method described by Hoffman (13). The *Escherichia coli* strains for the expression of L9 were generously provided by the Hoffman group.

Sample Preparation. An NMR sample for the pH titration of L9 was prepared in D_2O at a concentration of 1.8 mM in 10 mM phosphate and 100 mM sodium chloride. 3-(Trimethylsilyl) propionate (TSP) was used as an internal reference. A CD sample for the pH titration was prepared in D_2O containing 10 mM sodium phosphate and 100 mM sodium chloride. The protein concentration was $15 \mu\text{M}$. All solutions for stopped-flow fluorescence and stopped-flow CD experiments on L9 were prepared in H_2O or D_2O at a protein concentration of 1.3 mM in 20 mM sodium acetate and 100 mM sodium chloride and were adjusted to pH 5.45 for the samples in H_2O and to a pH meter reading of 5.05 for the sample in D_2O . The concentration of the sample of the

¹ Abbreviations: GdnHCl, guanidine hydrochloride; CD, circular dichroism; 1D, one-dimensional; NMR, nuclear magnetic resonance.

isolated N-terminal domain was 5.0 mM. Experiments in D₂O were carried out to allow a direct comparison with our previous study of the N-terminal domain and its truncation mutant.

Circular Dichroism Spectroscopy. The ellipticity at 222 nm was recorded at different pD values using an AVIV 62A DS spectrometer equipped with a Peltier temperature control unit. The signal from the sample in a 1 cm cuvette was averaged for 90 s. The pD was adjusted by adding NaOD or DCl directly to the cuvette. The readings on the pH meter were corrected for isotope effects and are referred as pD_{corr}. The measurements were performed at 25 °C.

Nuclear Magnetic Resonance (NMR). One-dimensional ¹H NMR spectra were obtained at different pD values using a Varian Instruments Inova 600 MHz spectrometer. The readings on the pH meter were corrected for isotope effects and are referred as pD_{corr}. The values of pD_{corr} were adjusted by adding NaOD or DCl. All experiments were conducted at 25 °C. Typically, 128 scans were collected using a recycle delay of 4.0 s. Residual HOD was suppressed by presaturation. The FIDs were 32K complex points and were zero-filled before Fourier transforming. No window function was applied.

Stopped-Flow Fluorescence. Stopped-flow fluorescence experiments were performed using an Applied Photophysics SX.18MV stopped-flow instrument. Fluorescence signals from Tyr 25 in the N-terminal domain and Tyr 126 in the C-terminal domain were measured with an excitation wavelength of 279 (±2) nm using a 305 nm cutoff filter. The temperature of the solutions and the flow circuit was maintained at 25 °C with a circulating water bath. For the pH jump experiments, a solution of L9 adjusted to pH 2.0 was rapidly diluted against 10 volumes of buffer solution adjusted to pH 7.5 in order to produce a final pH of 5.5. The final protein concentration was 50 μM. The curve was obtained by averaging 12 individual measurements and fit to a single-exponential function to determine a rate constant for the reaction. For the GdnDCl jump refolding experiments, L9 was unfolded in 6.8 M GdnDCl, and folding was initiated by 11-fold dilution into 0–4 M GdnDCl. For the unfolding experiments, L9 was unfolded by 11-fold dilution into 3–7 M GdnDCl. Each curve was obtained by averaging four to five individual measurements. The fast phase corresponding to the N-terminal domain was fit to a single exponential function to determine the apparent rate constant for the reaction. The slow phase was also separately fit to an exponential. The final protein concentrations were 50 μM. The dead time of the instrument was 3 ms.

Stopped-Flow CD. Stopped-flow CD measurements at 225 nm were made using an AVIV stopped-flow circular dichroism spectrometer model 202SF. For the pH jump experiments, a solution of L9 was adjusted to pH 2.0 and was rapidly diluted against 10 volumes of the folding buffer, which was adjusted to pH 7.5 in order to produce a final pH of 5.5. The decay curve was obtained by averaging 100 individual measurements and fit to a single-exponential function to determine the rate constant for the reaction. For the GdnHCl jump experiments, L9 was unfolded in 6.8 M GdnHCl, and folding was initiated by 11-fold dilution into 0–4 M GdnHCl. The unfolding experiments were initiated by 11-fold dilution into 3–7 M GdnHCl. Each curve was obtained by averaging 12–15 individual measurements. The

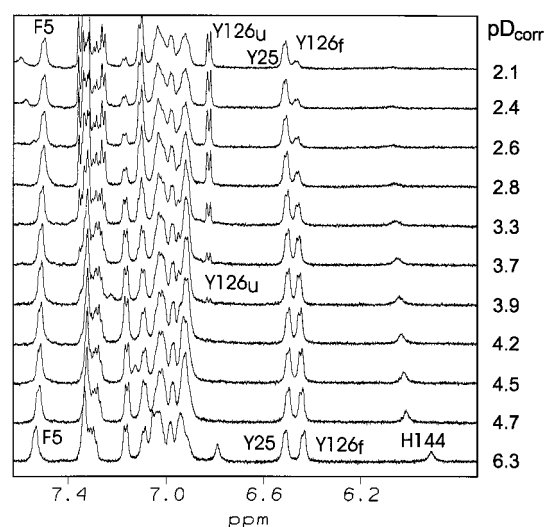


FIGURE 2: pD-dependent 1D ¹H NMR spectra of L9. The sample concentration was 1.8 mM L9 in 10 mM sodium phosphate, 100 mM sodium chloride, and 100% D₂O. Phe 5 and Tyr 25 are located in the N-terminal domain, and Tyr 126 and His 144 are in the C-terminal domain. The subscripts f and u refer to the resonance due to the proton in the folded state and in the unfolded state, respectively. The shift of the His 144 resonance between pD_{corr} 6.3 and pD_{corr} 4.7 is due to the protonation of the side chain.

fast phase and the slow phase were separately fit to a single-exponential function to determine the rate constants for each reaction. For both sets of experiments, the final protein concentration was 110 μM, and the temperature was maintained at 25 °C. The folding kinetics of the N-terminal domain in the intact protein and the isolated N-terminal domain were also measured in D₂O at 15 °C. L9 was unfolded in 5.9 M GdnDCl, and the folding was initiated by 5.5-fold dilution into 0.3 M GdnDCl. The trace was obtained by averaging 100 individual measurements. The isolated N-terminal domain was unfolded in 7.2 M GdnDCl, and the folding was initiated by 5.5-fold dilution into 0 M GdnDCl. The trace was obtained by averaging 20 individual measurements. The final protein concentration was 240 μM for L9 and 910 μM for the isolated N-terminal domain. The final GdnDCl concentration was 1.3 M for the both experiments. The dead time of the CD stopped-flow instrument was 6 ms.

Error Analysis. The uncertainty in the parameters obtained by nonlinear regression was estimated using the method described by Shoemaker (26). Treating one of the parameters as a constant, regressions were repeated to obtain a set of χ^2 values. An F-test then compared the newly obtained χ^2 values with the χ^2 value calculated from the best fit to determine the 95% confidence limit. The uncertainty in a parameter obtained from nonlinear regression is not necessarily symmetric. This analysis does not include cross correlation effects and thus provides an upper estimate of the uncertainty.

RESULTS

The C-Terminal Domain Unfolds at Low pH While the N-Terminal Domain Is Fully Folded. A series of 1D ¹H NMR spectra were recorded at different pD in order to observe pD-dependent effects on the stability of the two domains (Figure 2). The resonance assignments from Kuhlman (14) and Hoffman (12) were used to identify the resolved

resonances in the aromatic region. Peaks from Tyr 25 and Phe 5 in the N-terminal domain and from Tyr 126 and His 144 in the C-terminal domain could be followed. The spectra clearly show that the C-terminal domain starts to unfold around pD_{corr} 4.0 while the N-terminal domain is fully folded over the entire pD range. The resonance due to Tyr 126 from the folded protein (6.5 ppm) starts to decrease in intensity around pD_{corr} 4 at the same time as the resonance due to the same residue in the unfolded state starts to appear at 6.8 ppm. The observation of sharp separate resonances indicates that the two states are in slow exchange. The resonance due to His 144 from the folded protein also starts to disappear near pD_{corr} 4.0, although the resonance from the unfolded protein is not resolved in the 1D ^1H spectrum. The intensity of the His 144 resonance continues to decrease at low pD but can be still observed in the stacked plot upon magnification. This pattern of pH-dependent spectral changes indicates that the C-terminal domain starts to unfold around pD_{corr} 4.0. The Tyr 126 resonance due to the folded state has not completely disappeared at pD_{corr} 2.1, which indicates that the C-terminal domain is not completely unfolded at low pD . The ratio of the integrals of the folded resonance and unfolded resonance of Tyr 126 shows that approximately 25% of the molecules are still folded at pD_{corr} 2.1. The resonances due to Tyr 25 and Phe 5, which are both in the N-terminal domain, are independent of pD . Since the folding rate of the N-terminal domain is intermediate to fast on the NMR time scale, the resonances would have shifted and broadened if the domain unfolded (14, 25). Thus, the N-terminal domain is completely folded even at pD_{corr} 2.1. This result is expected since the isolated N-terminal domain has been shown to be stable to at least pH 1.0 (27).

The acid-induced unfolding of the C-terminal domain was also monitored by following the CD signal at 222 nm (Figure 3), and similar results were obtained. The helical content starts to decrease at around pD_{corr} 4.0 but still remains high at pD_{corr} 2.0. The 25% of the molecules which contains a folded C-terminal domain cannot account for all of the observed signal at pD_{corr} 2.0, suggesting that the N-terminal domain is structured. There is also likely to be a contribution from the central helix since the isolated helix is known to partially folded at low pH at 25 °C (11). Assuming that 25% of the molecules have a folded C-terminal domain at pD_{corr} 2.0, the transition followed by CD overlaps very well with the transition monitored by NMR (Figure 3), providing evidence that the acid-induced unfolding of the C-terminal domain is two state. Thus, the NMR and CD data indicate that the C-terminal domain unfolds at low pH while the N-terminal domain is still fully folded. This opens the possibility of performing pH jump experiments to study the folding of the C-terminal domain under conditions where the N-terminal domain is folded. In the next section, we compare the results of CD detected GdnHCl jump experiments with fluorescence-detected GdnHCl jump experiments. This comparison provides an excellent test of the apparent two-state folding of the domains. We then compare the results of the GdnHCl jump experiments to pH jump measurements.

GdnHCl Jump Experiments Using Stopped-Flow CD and Stopped-Flow Fluorescence Provide Evidence for Two-State Folding. The stopped-flow CD traces obtained from GdnHCl jump experiments showed two well-resolved exponential

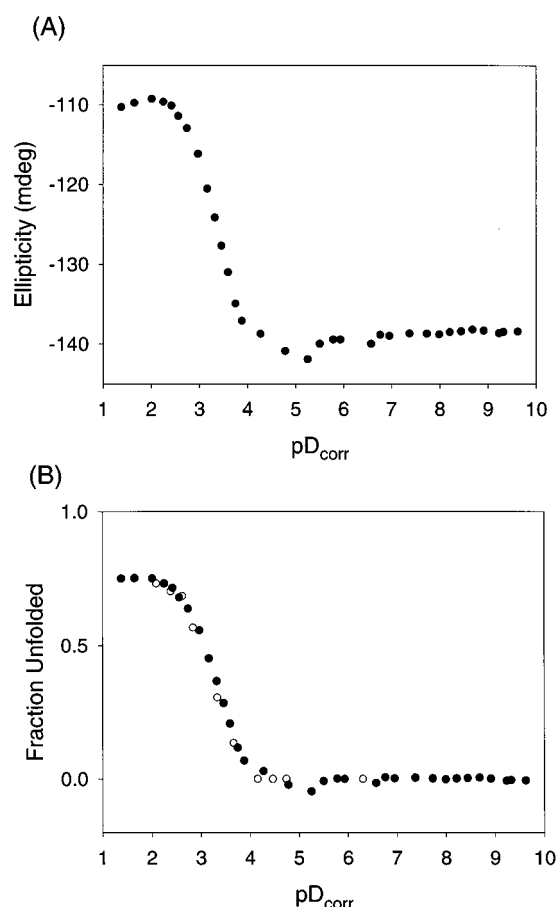


FIGURE 3: (A) Acid-induced unfolding of L9 monitored by CD at 222 nm. The sample concentration was 15 μM L9, in 10 mM sodium phosphate, and 100 mM sodium chloride in D_2O . (B) Apparent fraction unfolded of the C-terminal domain calculated from the CD data (closed circles) and from the intensity of the Tyr 126 NMR resonances (open circles).

phases. A representative trace is shown in Figure 4. The observation of two well-resolved phases is similar to what we observed in our previous fluorescence detected stopped-flow experiments. Using information from NMR line-shape analysis and saturation transfer experiments, the fast phase was assigned to the N-terminal domain, and the slow phase was assigned to the C-terminal domain (25). Therefore, the rapid initial decay (to more negative values) of the CD signal is assigned to the N-terminal domain, and the slow decrease is assigned to the C-terminal domain. The two phases were well enough resolved to allow them to be fit independently.

Kinetic data are commonly presented as a plot of the natural logarithm of observed rate constants versus denaturant concentration, a so-called chevron plot. If a protein folds in a two-state fashion, the folding and unfolding branches of the chevron plot are linear while the presence of an intermediate typically leads to rollover in the plot (28). For both the N-terminal domain and the C-terminal domain, the chevron plots derived from the CD experiment show a v-shaped curve and overlap well with the plots from our previous fluorescence experiments (Figure 5). The absence of any rollover in either chevron plot, together with the excellent agreement between the fluorescence and CD detected experiments, provides strong evidence for the independent two-state folding of each domain. The chevron plots were fit to the following equation to determine the

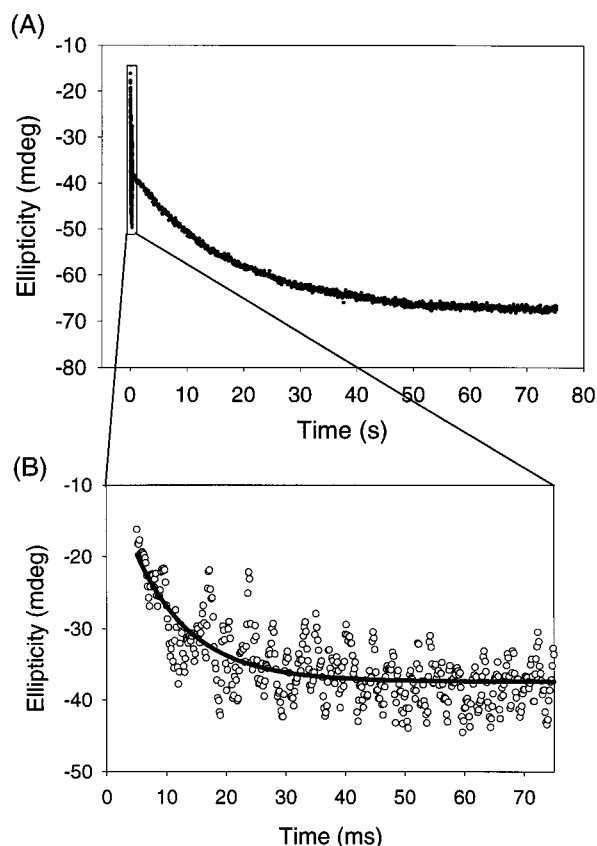


FIGURE 4: Representative folding trace obtained from the stopped-flow CD experiments by a GdnHCl jump. The final GdnHCl concentration was 1.3 M, and the pH was 5.45. (A) The complete trace. (B) An expansion of the initial portion of (A). The initial part of the trace shown in panel A is well fit to a single-exponential function as is the longer time decay.

folding and unfolding rate constants in the absence of GdnHCl [k_f (0 M GdnHCl) and k_u (0 M GdnHCl)]

$$\ln(k_{\text{obs}}) = \ln[k_f(0 \text{ M GdnHCl}) \exp(m_f[\text{GdnHCl}]/RT) + k_u(0 \text{ M GdnHCl}) \exp(m_u[\text{GdnHCl}]/RT)] \quad (1)$$

where k_{obs} is an observed rate constant, and m_f and m_u are constants that describe how k_f and k_u vary as a function of the concentration of GdnHCl. The results are listed in Table 1. The folding rate constants in the absence of GdnHCl were determined to be 760 s^{-1} for the N-terminal domain and 4.7 s^{-1} for the C-terminal domain. The rates measured by stopped-flow CD show an excellent agreement with the results from the fluorescence experiments (760 s^{-1} for the N-terminal domain and 3.0 s^{-1} for the C-terminal domain).

The compactness of the transition state for folding can be obtained from analysis of the slope of the folding branch ($m_f R^{-1}T^{-1}$) and the slope of the unfolding branch ($m_u R^{-1}T^{-1}$) of the chevron plot (29, 30). The values of m_f and m_u are related to the change in solvent accessible surface area between the initial states and the transition state. The difference ($m_u - m_f$), for a two-state folding protein, is equal to the m value measured in an equilibrium denaturation experiment. The ratio of m_f to the equilibrium m value referred to as θ_m is a measure of the position of the transition state in terms of solvent exposure (29). A value of θ_m close to 1 indicates that the transition state is nativelike in terms of solvent-accessible surface area, and a smaller value of

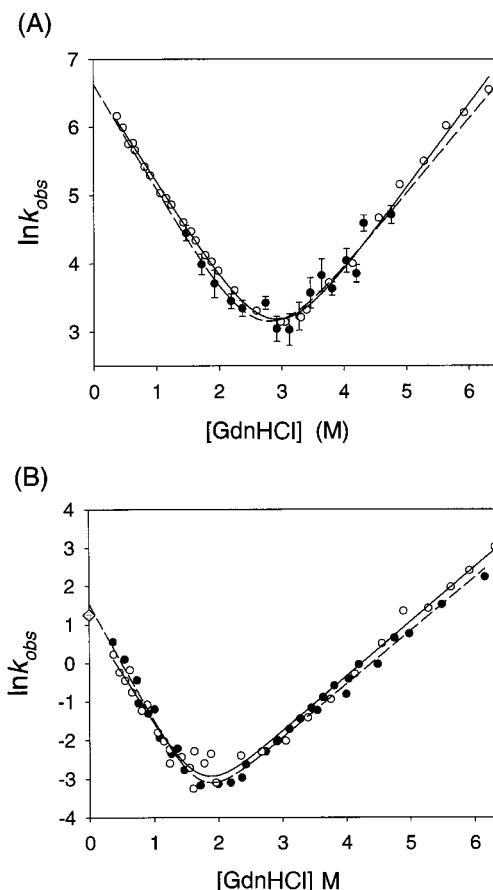


FIGURE 5: Plots of the natural logarithm of the observed rate constants versus GdnHCl concentration. Open circles and solid lines are from the stopped-flow fluorescence experiments of Sato et al. (25). Closed circles and broken lines are from the stopped-flow CD experiments. (A) The N-terminal domain. The solid and broken lines are the best fits to eq 1 giving a k_f of 760 and 760 s^{-1} by CD and fluorescence, respectively. (B) The C-terminal domain. The solid and broken lines are the best fits to eq 1 giving a k_f of 3.0 and 4.7 s^{-1} by fluorescence and CD, respectively. The shaded diamond represents the results from the pH jump experiments using CD and fluorescence detection. The same rate was obtained with both techniques. The uncertainties corresponding to 95% confidence limits for the stopped-flow CD data are shown as error bars in panel A and are approximately the same as the size of the circles in panel B. The uncertainties associated with all of the stopped-flow fluorescence data are less than the size of the circles.

θ_m indicates that the transition state is more like the denatured state. The calculated θ_m values from the stopped-flow CD measurements are 0.6 for the N-terminal domain and 0.7 for the C-terminal domain, which are also in good agreement with the results from fluorescence measurements.

pH Jump Experiments. The folding rate constant of the C-terminal domain was measured by pH jump experiments performed in the absence of denaturant. These experiments can be performed starting from conditions where the N-terminal domain is folded and thus allow us to probe how the presence or absence of structure in the N-terminal region of the molecule affects the folding of the C-terminal region. Folding was initiated by rapidly jumping the pH from 2.0 to 5.5. Both stopped-flow fluorescence and CD experiments were conducted. The fluorescence and the CD traces showed an exponential decrease on the expected time scale for the folding of the C-terminal domain (Figure 6). As expected, the fast phase corresponding to the folding of the N-terminal domain (a folding rate constant of 760 s^{-1}) was absent in

Table 1: Comparison of the Kinetic Parameters Obtained by Stopped-Flow CD and Stopped-Flow Fluorescence^a

	N-terminal domain in intact L9		Isolated N-terminal domain	C-terminal domain in intact L9			
	CD GdnHCl jump ^b	fluorescence GdnHCl jump ^c	fluorescence GdnHCl jump ^d	CD		fluorescence	
				GdnHCl jump ^b	pH jump ^b	GdnHCl jump ^c	pH jump ^b
k_f (s ⁻¹)	760 (+6800, -600)	760 (+180, -140)	720 (+280, -190)	4.7 (+6.1, -2.6)	3.5 (+2.5, -1.1)	3.5 (+8.0, -2.2)	3.5 (+0.1, -0.1)
k_u (s ⁻¹)	0.63 (+7.27, -0.62)	0.36 (+0.28, -0.18)	0.75 (+0.74, -0.39)	0.0023 (+0.025, -0.0022)		0.0025 (+0.026, -0.0023)	
ΔG° (kcal mol ⁻¹)	4.21 (+2.29, -1.41)	4.53 (+0.36, -0.32)	4.06 (+0.45, -0.41)	4.51 (+0.72, -0.75)		4.23 (+0.80, -0.71)	
θ_m	0.59 (+0.29, -0.39)	0.54 (+0.05, -0.05)	0.60 (+0.07, -0.07)	0.69 (+0.12, -0.13)		0.65 (+0.12, -0.13)	

^aNumbers in parentheses correspond to the 95% confidence limit. All experiments were performed at 25 °C in 20 mM sodium acetate, 100 mM sodium chloride. After mixing, the final pH was 5.5 for all experiments. ^bFrom this work. ^cFrom Sato et al. (25). ^dFrom Kuhlman et al. (31).

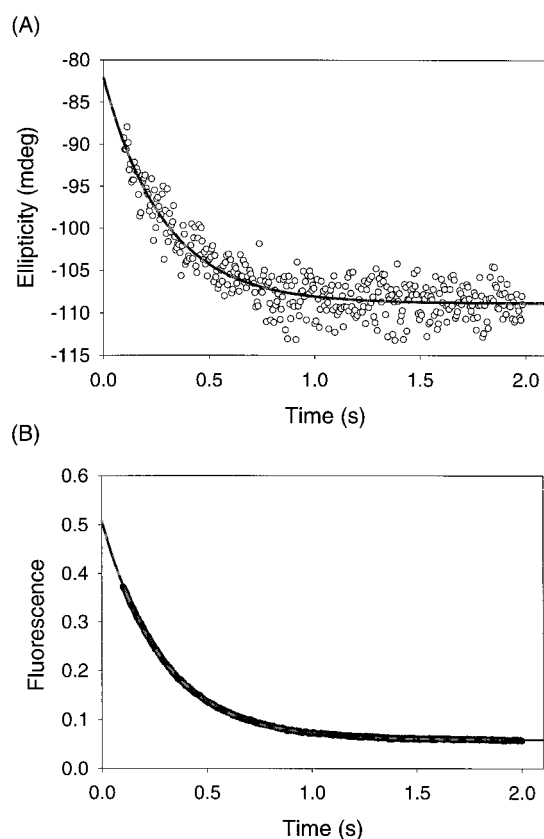


FIGURE 6: Stopped-flow traces for the C-terminal domain obtained by the pH jump experiments. (A) CD detected trace. (B) Fluorescence detected trace. The curves are the resulting best fits to a single-exponential function giving a k_f of 3.5 s⁻¹ for both traces. The initial pH was 2.0, and the final pH was 5.5.

all the profiles. The rate constants obtained from the fluorescence experiments and the CD experiments were 3.5 s⁻¹ (+0.1, -0.1) and 3.5 s⁻¹ (+2.5, -1.1), respectively. These values agree with each other and with the values determined from the GdnHCl jump experiments (3.0 s⁻¹ from the fluorescence experiments, 4.7 s⁻¹ from the CD experiments). These results indicate that the folding rate of the C-terminal domain is not affected by the folding status of the N-terminal domain. Since the N-terminal domain is fully folded before and after the pH jump, it is highly unlikely that parts of the peptide chain corresponding to the N-terminal domain interfere with the folding of the C-terminal domain. The agreement of the rate constants measured by the pH jump experiments and the GdnHCl jump experiments,

Table 2: Comparison of the Kinetic Parameters for the N-Terminal Domain in the Intact Protein, the Isolated N-Terminal Domain (1–56) and the Truncated Version of the Isolated N-Terminal Domain (1–51)^a

	N-terminal domain in the intact protein in D ₂ O	Isolated N-terminal domain (1–56) in D ₂ O	Isolated N-terminal domain (1–51) in D ₂ O
k_f (s ⁻¹)	1110 (-230, +300)	1053 (-277, +213)	942 (-328, +235)
k_u (s ⁻¹)	0.42 (-0.22, +0.40)	0.55 (-0.40, +0.24)	6.50 (-2.0, +1.7)
ΔG° (kcal mol ⁻¹)	4.67 (-0.35, +0.38)	4.47 (-0.50, +0.50)	2.95 (-0.18, +0.20)
m (kcal mol ⁻¹ M ⁻¹)	1.59 (-0.07, +0.09)	1.47 (-0.14, +0.14)	1.49 (-0.08, +0.08)
θ_m	0.58 (-0.05, +0.06)	0.59 (-0.05, +0.05)	0.71

^a All experiments were performed at 25 °C in D₂O, 20 mM sodium acetate, 100 mM NaCl, pD_{corr} 5.45. The data for the isolated N-terminal domain (1–56) and the 1–51 variant were taken from Luisi et al. (32). The numbers in brackets represent the 95 % confidence limit.

therefore, suggests that the slow folding of the C-terminal domain is not due to unfavorable interactions with the rest of the protein.

Kinetic Measurements in D₂O Allow the Comparison of the Folding Rate of the N-Terminal Domain in L9 to the Folding Rate of the Isolated N-Terminal Domain. We have previously determined the folding rates of two variants of the isolated N-terminal domain. One construct corresponds to residues 1–56, while the other was comprised of residues 1–51 (14, 31). These experiments were conducted in D₂O to allow the combined analysis of stopped-flow and NMR measurements. It is well-known that proteins are generally more stable in D₂O. Thus, it is not possible to directly compare the folding rates measured for intact L9 in H₂O to these measured for the isolated domain in D₂O. Consequently, we have also measured the folding rate of L9 in D₂O by fluorescence detected stopped-flow. A chevron plot for the N-terminal domain was obtained and showed a v-shape curve (data not shown). Results obtained by curve fitting to eq 1 are listed in Table 2 and compared with the parameters for the two variants of the isolated N-terminal domain. The folding and unfolding rate constants in the absence of denaturant were calculated to be 1110 and 0.44 s⁻¹, respectively, and the value of θ_m was found to be 0.58. The measured rate constants correspond to a ΔG° of 4.67 kcal mol⁻¹, which indicates that the apparent stability of the

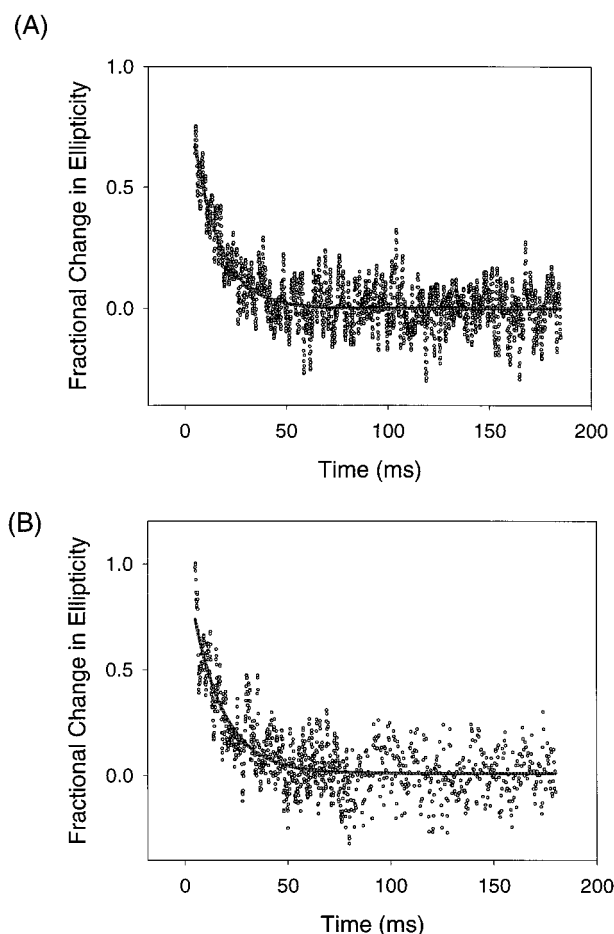


FIGURE 7: Comparison of the GdnDCl jump stopped-flow CD trace of the N-terminal domain in the intact domain (A) and the isolated N-terminal domain (B). The final GdnDCl concentration was 1.3 M in both cases. The curves are the best fits to a single-exponential function giving a k_f of 78 s^{-1} for the domain in the intact protein and 63 s^{-1} for the isolated domain. The signals at 225 nm were recorded in D_2O at 15°C and were normalized by setting the signal from the unfolded state as 1 and the signal from the folded state as 0.

N-terminal domain of L9 is slightly higher in D_2O than in H_2O (the value of ΔG° in H_2O is $4.53 \text{ kcal mol}^{-1}$). The increase in stability is slightly less than that measured for the isolated domain (31).

Stopped-Flow CD Measurements of the Folding of the Isolated N-Terminal Domain. We have also used stopped-flow CD to measure the folding kinetics of the isolated N-terminal domain. Unfortunately, the rapid folding of the protein and the low signal-to-noise ratio of this experiment prevented collection of the entire chevron plot. Instead, we compare the folding rates under conditions where the observed rate constant is dominated by the folding rate. GdnHCl jump experiments were conducted in which the final denaturant concentration was 1.3 M.

The stopped-flow CD trace of the N-terminal domain in the intact protein is compared to the trace of the isolated N-terminal domain in Figure 7. Both profiles show a rapid decay of the CD signal which can be fit by a single-exponential giving a measured rate constant of 78 s^{-1} for the N-terminal domain in the intact protein and 63 s^{-1} for the isolated domain. Given the inherently noisy nature of the data, the observed rates agree well with each other. This agreement suggests that rate of formation of secondary

structure in the isolated N-terminal domain is essentially the same as that for the N-terminal domain in the intact protein.

DISCUSSION

All the results obtained in this study indicate that both the N-terminal domain and the C-terminal domain fold via a simple two-state process. For both of the domains, the plots of $\ln(k_{\text{obs}})$ versus GdnHCl concentration obtained from the stopped-flow CD experiments show the expected V-shaped curve for two-state folding and overlap well with the plots obtained from fluorescence experiments. The additional data points collected at 0 M GdnHCl from the pH jump experiments are included in the chevron plot shown in Figure 5. These data clearly demonstrate that there is no deviation from linearity at low denaturant concentration and eliminate the possibility of any rollover. The overlap of the curves determined by the two different techniques gives strong evidence for the two-state folding of each domain. The large difference in the folding rates of the N-terminal domain and the C-terminal domain indicates that the folding of the two domains is not kinetically coupled. Our results imply that the folding process of L9 is dictated by two separate hydrophobic cores: one in the N-terminal domain and the other in the C-terminal domain. The good agreement of the stopped-flow CD traces of the N-terminal domain in the intact protein and the isolated N-terminal domain provides additional evidence that the folding process of the isolated domain is the same as the folding of the domain in the intact protein.

The C-terminus of the N-terminal domain corresponds to the start of the connecting helix which links the N- and C-terminal domains of L9. Extending the length of this helix has no effect on the folding rate of the N-terminal domain. Constructs corresponding to residues 1–51 and residues 1–56 have been shown to fold at the same rate even though they differ in stability and have drastically different propensities to populate helical structure in their unfolded states (32). The fact that the N-terminal domain of the intact protein also folds with the same rate confirms that formation of all or part of the connecting helix does not play a role in the rate-limiting step for the formation of the N-terminal domain. Comparison of the kinetic parameters for the three proteins suggests an inverse correlation between the position of the transition state for folding and the stability of the N-terminal domain. The value of ΔG° is noticeably smaller for the 1–51 residue variant, and this protein has a θ_m value of 0.71. The stability of the 1–56 variant is very similar to the apparent stability of the N-terminal domain of intact L9, and the values of θ_m are essentially identical for these two proteins, 0.58 and 0.59, respectively.

The folding rate of the N-terminal domain of L9 shows an excellent agreement with the value predicted by the relative contact order as does the value of θ_m . The relative contact order of the N-terminal domain is 12.7% corresponding to a predicted folding rate constant of 1900 s^{-1} . The predicted rate and measured rate are in very good agreement, especially considering that experimentally determined folding rates vary by a factor of 10^6 . The experimentally determined values of θ_m for the C-terminal domain is in good agreement with the value predicted by the relative contact order. Interestingly, the folding rate for the C-terminal domain

predicted by the contact order analysis deviates from that observed experimentally by a factor of 35–100. This is one of the largest reported deviations of measured and predicted rates. This disagreement might be explained if the domain folds slower in the intact protein because of unfavorable interactions with the rest of protein during the folding. The pH jump experiments, however, demonstrate that the folding rate of the C-terminal domain is not affected by the folding status of the N-terminal domain. This result suggests that the N-terminal region of the protein is not likely to influence the folding of the C-terminal domain. The analysis of Goddard and co-workers more accurately predicts the folding rate of the C-terminal domain of L9. The method is, however, not perfect since it noticeably underestimates folding rates for all-helical proteins. In contrast, the folding rates for helical proteins are accurately predicted by contact order analysis. The discovery of the correlation between the relative contact order and folding rates has contributed significantly to the prediction of the folding rates, but there are likely other factors which remain to be elucidated. The results presented here indicate that the isolated C-terminal domain of L9 is an interesting subject for further study.

ACKNOWLEDGMENT

We thank Dr. Brian Kuhlman and Professor Kevin Plaxco for numerous helpful discussions and for calculating the relative contact order of the two domains of L9 as well as for their continued interest in this work. We thank Professor David Hoffman for generously providing us with the *E. coli* strains for the production of L9 and with the coordinates of L9 prior to publication.

REFERENCES

1. Anfinsen, C. B. (1973) *Science* 181, 223–230.
2. Levinthal, C. (1968) *J. Chim. Phys.* 65, 44–45.
3. Dill, K. A., Bromberg, S., Yue, K., Fiebig, K. M., Yee, D. P., Thomas, P. D., and Chan, H. S. (1995) *Protein Sci.* 4, 561–602.
4. Jackson, S. E. (1998) *Folding Des.* 3, R81–R91.
5. Plaxco, K. W., Simons, K. T., and Baker, D. (1998) *J. Mol. Biol.* 277, 985–994.
6. Debe, D. A., and Goddard, W. A. I. (1999) *J. Mol. Biol.* 294, 619–626.
7. Abkevich, V. I., Gutin, A. M., and Shakhnovich, E. I. (1995) *Protein Sci.* 4, 1167–1177.
8. Price, N. C. (1994) in *Mechanisms of Protein Folding* (Pain, R. H., Ed.), Oxford University Press, Oxford, U.K.
9. Jaenicke, R. (1991) *Biochemistry* 30, 3147–3161.
10. Lillemoen, J., Cameron, C. S., and Hoffman, D. W. (1997) *J. Mol. Biol.* 268, 482–493.
11. Kuhlman, B., Yang, H. Y., Boice, J. A., Fairman, R., and Raleigh, D. P. (1997) *J. Mol. Biol.* 270, 640–647.
12. Hoffman, D. W., Cameron, C. S., Davies, C., White, S. W., and Ramakrishnan, V. (1996) *J. Mol. Biol.* 264, 1058–71.
13. Hoffman, D. W., Davies, C., Gerchman, S. E., Kycia, J. H., Porter, S. J., White, S. W., and Ramakrishnan, V. (1994) *EMBO J.* 13, 205–212.
14. Kuhlman, B., Boice, J. A., Fairman, R., and Raleigh, D. P. (1998) *Biochemistry* 37, 1025–1032.
15. Kuhlman, B., Luisi, D. L., Evans, P. A., and Raleigh, D. P. (1998) *J. Mol. Biol.* 284, 1661–1670.
16. Vugmeyster, L., Kuhlman, B., and Raleigh, D. P. (1998) *Protein Sci.* 7, 1994–1997.
17. Wittung-Stafshede, P., Lee, J. C., Winkler, J. R., and Gray, H. B. (1999) *Proc. Natl. Acad. Sci. U.S.A.* 96, 6587–6590.
18. Spector, S., and Raleigh, D. P. (1999) *J. Mol. Biol.* 293, 763–768.
19. Mines, G. A., Pascher, T., Lee, S. C., Winkler, J. R., and Gray, H. B. (1996) *Chem. Biol.* 3, 491–497.
20. Huang, G. S., and Oas, T. G. (1995) *Proc. Natl. Acad. Sci. U.S.A.* 92, 6878–6882.
21. Schindler, T., Herrler, M., Marahiel, M. A., and Schmid, F. X. (1995) *Nat. Struct. Biol.* 2, 663–673.
22. Khorasanizadeh, S., Peter, I. D., Butt, T. R., and Roder, H. (1993) *Biochemistry* 32, 7054–7063.
23. Parker, M. J., Spencer, J., Jackson, G. S., Burston, S. G., Hosszu, L. L., Craven, C. J., Waltho, J. P., and Clarke, A. R. (1996) *Biochemistry* 35, 15740–15752.
24. Jaenicke, R. (1999) *Prog. Biophys. Mol. Biol.* 71, 155–241.
25. Sato, S., Kuhlman, B., Wu, W. J., and Raleigh, D. P. (1999) *Biochemistry* 38, 5643–5650.
26. Shoemaker, D. P., Garland, C. W., and Nibler, J. W. (1989) *Experiments in Physical Chemistry*, 5th ed., McGraw-Hill Inc, New York.
27. Kuhlman, B., Luisi, D. L., Young, P., and Raleigh, D. P. (1999) *Biochemistry* 38, 4896–4903.
28. Baldwin, R. L. (1996) *Folding Des.* 1, R1–R8.
29. Tanford, C. (1970) *Adv. Protein Chem.* 24, 1–95.
30. Tanford, C. (1968) *Adv. Protein Chem.* 23, 121–282.
31. Kuhlman, B., and Raleigh, D. P. (1998) *Protein Sci.* 7, 1–8.
32. Luisi, D. L., Kuhlman, B., Sideras, K., Evans, P. A., and Raleigh, D. P. (1999) *J. Mol. Biol.* 289, 167–174.
33. Kraulis, P. J. (1991) *J. Appl. Crystallogr.* 24, 946–950.

BI992608U